Results of a Precrash Application Based on Laser Scanner and Short-Range Radars

Sylvia Pietzsch, Trung-Dung Vu, Julien Burlet, Olivier Aycard, Thomas Hackbarth, Nils Appenrodt, Jurgen Dickmann, Bernd Radig

Results of a Precrash Application based on Laser Scanner and Short Range Radars

Sylvia Pietzsch, Trung Dung Vu, Julien Burlet, Olivier Aycard, Thomas Hackbarth, Nils Appenrodt, Jürgen Dickmann, and Bernd Radig

***Abstract*—In this paper, we present a vehicle safety application based on data gathered by a laser scanner and two short range radars that recognizes unavoidable collisions with stationary objects before they take place in order to trigger restraint systems. Two different software modules are compared that perform the processing of raw data and deliver a description of the vehicle's environment. A comprehensive experimental evaluation based on relevant crash and non-crash scenarios is presented.**

***Index Terms*—Road vehicles, sensor fusion, perception system, collision mitigation.**

I. Introduction

In recent years, a lot of research has been done to develop safety applications which help to prevent accidents or mitigate their consequences [1]. The automatic recognition of imminent collisions plays an important role in making traffic safer [2] [3]. The earlier a potential collision is detected, the more possibilities are available to protect car passengers and other road users. In this document, we describe a system to detect frontal collisions. In case a crash is predicted to happen within the next 200 milliseconds, the system triggers reversible belt pretensioners which bring the passenger into an upright position that is safer during the crash and removes the belt slack in advance. An experimental vehicle was equipped with sensors and processing hardware to demonstrate the operational capability of the safety function in real time.

The perception of the environment in front of the vehicle is based on data from a laser scanner and two short range radars. The advantages of the laser scanner are its large field of view and its high angular and range resolution and accuracy. Labayrade et al. [3], for example, fuse objects from a laser scanner with objects from a stereovision system for emergency braking. Other approaches for collision detection rely on a combination of stereovision and radar, e.g. [4]. Radar sensors are in common use for driver assistant systems in cars and complement our system due to immediate velocity measurements and the use of a complementary emission type.

The methods and software modules presented in this paper were developed within the Integrated Project PReVENT, a European research activity to contribute to road safety by developing preventive safety applications and technologies, co-funded by the European Commission. The presented work comprises two different software modules for sensor data processing that were developed independently by the Daimler AG (Module 1) and LIG & INRIA Rhônes Alpes (Module 2). The perception module 1 and the precrash application are part of the research done within APALACI (Advanced Pre-crash And LongitudinAl Collision mitigation), a subproject of PReVENT with the objective of protecting vehicle occupants. Perception module 2 was developed within the framework of PROFUSION2, a subproject that aims at developing concepts and methods for different sensor data fusion approaches as an enabler for advanced vehicle safety and assistance functions.

Module 1 utilizes grid-based segmentation of the laser scanner data and Kalman filter techniques to track objects. Module 2 is based on simultaneous localization and mapping techniques (SLAM) together with the detection and tracking of moving objects. The environment is modeled using an Occupancy Grid. Detected moving objects are tracked by a Multiple Hypothesis Tracker (MHT) coupled with an adaptive Interacting Multiple Models filter (IMM). Our evaluation compares the performance of both modules on the basis of the output of a shared precrash decision module by means of missed and false alarm rates in complex crash and non-crash maneuvers with stationary objects, respectively.

The remainder of this paper is organized as follows: In Section II the experimental vehicle together with the sensors are described. Section III and Section IV deal with the technical and scientific background of sensor data processing. They give an overview over the methods that are used within each of the modules for environmental perception. Section V explains subsequent processing steps that perform situation analysis and the decision for or against a collision. Test results in various driving scenarios are presented in Section VI. Finally, Section VII summarizes the presented content and gives suggestions for further work.

II. Experimental Vehicle and Sensors

The experimental vehicle, a Mercedes-Benz E-Class, is equipped with an Ibeo "ALASCA" laser scanner mounted

Manuscript received Sept 1, 2008; revised March 2, 2009. This work was supported in part by the Information Society of the European Union under the Contract No. 507075 in the framework of the integrated Project PReVENT.

S. Pietzsch is with the Technische Universität München, Chair for Image Understanding and Knowledge-based Systems and works cur. for the Daimler AG, 89081 Ulm, Germany (e-mail: uni-muenchen.pietzsch@daimler.com).

T. D. Vu, J. Burlet and O. Aycard are with the Laboratoire d'Informatique de Grenoble and INRIA Rhônes Alpes, Grenoble, France (e-mail: tdvu@inrialpes.fr, jburlet@inrialpes.fr, olivier.aycard@inrialpes.fr).

T. Hackbarth, N. Appenrodt and Dr. J. Dickmann are with the Department for Environment Perception, Research Centre of the Daimler AG, 89081 Ulm, Germany (e-mail: thomas.hackbarth@daimler.com, nils.appenrodt@daimler.com, juergen.dickmann@daimler.com).

B. Radig is with the Technische Universität München, Chair for Image Understanding and Knowledge-based Systems, Garching, Germany.

TABLE I
TECHNICAL DATA OF THE SENSORS

Property	Laser scanner	Short range radar
Angle	160°	80°
Angle accuracy	+/-0.5°	+/-5..10°
Range	0.3-80 m	0.2-30 m
Range accuracy	+/-5 cm	+/-7.5 cm
Scan frequency	25 Hz	25 Hz

below the number plate and two M/A-COM "SRS100" 24 GHz short range radar prototypes mounted in the front bumper besides the number plate. The laser scanner is hermetically covered by a box having a black plastic faceplate which is transparent for the emission wavelength while the radars are mounted behind the standard plastic bumper. The technical specifications of the sensors are listed in Table I.

The radar sensors and the laser scanner controller are connected to a controller unit in the trunk by private CAN and Ethernet, respectively. This real time unit hosts a 366 MHz Motorola Power-PC processor which runs the software for sensor data processing, segmentation, object generation, tracking, sensor data fusion and activation decision.

In case of unavoidable collisions the reversible seatbelt pretensioners of the front seats are deployed via a private CAN. An additional PC in the trunk acts as a display server connected to a monitor in front of the passenger seat to visualize the environment perception and the activation decision. The architecture of the vehicle is shown in Fig. 1.

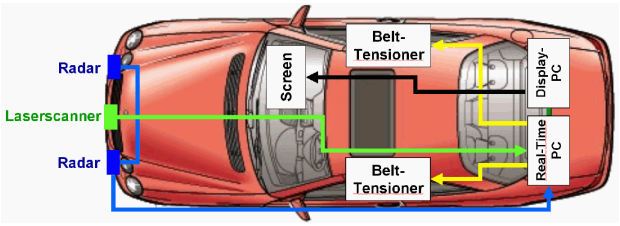

Fig. 1. Hardware architecture of the experimental vehicle showing sensors, actuators, computers and interconnects.

Fig. 2 shows a cutout of the screen exactly at the moment of deployment when the car approaches a foam cube with a constant speed of 50 km/h. On the screen, the targets seen by the laser scanner and the radars are shown as small dots and circles, respectively. The colors symbolize the mounting side of the radars and accordingly the four vertical beam layers of the laser scanner. Object segments, generated from the scanner targets, are depicted as rectangles. The actual TTC (time to collision) of 174 ms corresponds to a distance of 2.4 m. The inset of the figure shows the appropriate picture captured by the in-vehicle camera which is used for documentation purposes only.

III. PERCEPTION MODULE 1: POLAR GRID-BASED SEGMENTATION AND MID-LEVEL FUSION

This section and Section IV describe the mode of operation of the two different modules which perform the signal

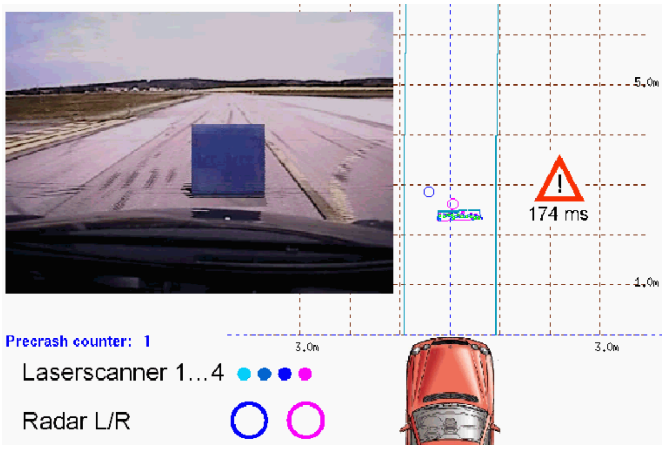

Fig. 2. Visualization of the environment perception on the in-vehicle screen. The inset shows the scene recorded by the camera behind the windshield.

processing of the individual sensors and their fusion. The result from either module is a description of the subject vehicle's surrounding environment with static and moving objects contained in it. Based on the state (position, velocity, direction, dimension and orientation) that the module estimates for each object relative to the subject vehicle, the application decides, whether an inevitable collision will take place within the next 200 ms. Furthermore, the precrash application is dealing with suppression of ghost targets and a plausibility check to ensure a robust system behavior.

Grid-based methods have proven to be efficient to process raw data provided by a laser scanner. In this module, developed at the Daimler AG, a grid approach is used for segmentation of laser scan points [5]. The segmentation grid is designed according to the scanner's measuring method. Scan points are processed in polar coordinates. Therefore, a radial grid is used whose dimensions denote angle and distance. The cell size increases with the distance from the scanner and the absolute value of the angle, thus enabling a good segmentation even in cases when some target points are lost near the border of the field of view due to low reflected intensity. Fig. 3 depicts a schematic representation of the segmentation grid. In the very near field, the parameterization of the grid can differ from the remaining grid area in order not to split objects in consequence of very narrow cells. Note that cell sizes as well as near and far field borders are not to scale. Cell sizes are widened due to better visibility.

The grid design influences the segmentation quality. Ideally, a segment should not contain more than one real object and an object should not split up into several segments. Therefore, the dimensions of the grid cells have to be chosen carefully. If the grid cells are too large, neighboring objects tend to be merged to one segment. Otherwise, if the grid cells are too small, a compact object splits into many small segments. Knowledge on the properties of expected traffic participants helps to find a suitable grid design. Inspecting a target vehicle driving parallel to the subject vehicle at a certain lateral distance the distance between measurement points from subsequent laser rays can be calculated given the scanner's angular resolution. These distances build the basis for longitudinal grid cell dimensions.

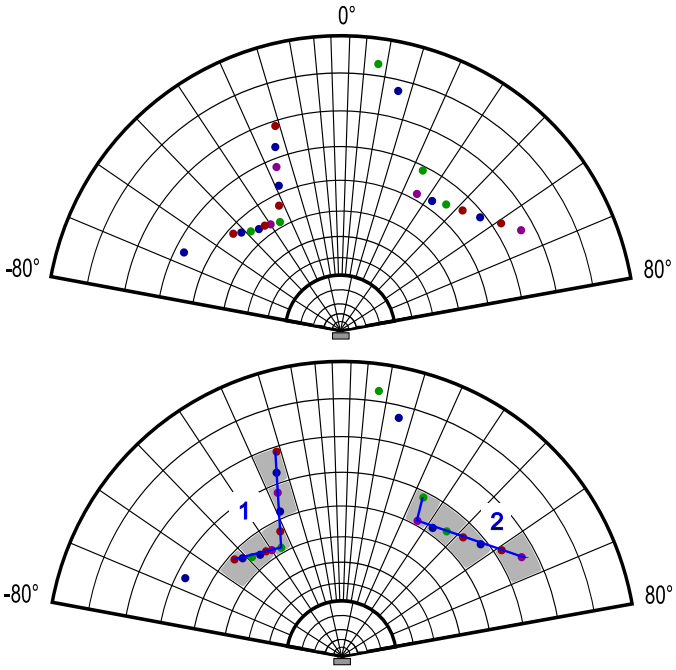

Fig. 3. Schematic grid design (not to scale) and segmentation procedure. Top: Projection of all scan points onto the grid. Bottom: Marking of grid cells with no. of points $\geq$ threshold, connecting of adjacent grid cells and labeling.

Laterally, the cell dimension is set to the physical scanner resolution at the center of field of view and increases towards the borders.

In scan segmentation algorithms, there is always a tradeoff between splitting objects that are located close together and merging objects that are split into different point clouds due to missing scan points [6]. Processing single frames without previous knowledge cannot resolve this ambiguity. Nevertheless, the presented method performs moderately well for the desired application, even with different sized targets.

All scan points of all four vertical layers of the laser scanner are projected onto the grid. If the number of measurements within a grid cell exceeds a given threshold the cell is marked as occupied. Neighboring occupied cells are connected to form one segment, afterwards. The procedure is illustrated in Fig. 3. Projecting all scan points onto a one-layered grid no matter which scan layer they originate from makes the process efficient in terms of computing time without too much information loss. Processing each layer separately is also possible, but in this case, complex logic is needed to combine the segmentation results from the different layers.

From the obtained segments, features that describe the properties of an object like dimension or orientation angle can be extracted. For feature extraction, the minimum angle point, the point with the shortest distance to the scanner and the maximum angle point are used to calculate a rectangular bounding box. The orientation angle denotes the angle between the longer of the two sides of a segment and the x-axis of the car coordinate system. As reference point the center of gravity of all points belonging to one segment is chosen.

The measurements of the laser scanner and the short range radars are combined using a midlevel fusion approach which is illustrated in the structure within the large frame in Fig. 4. Laser scanner data is processed in the way described above. The radar sensors deliver filtered and pretracked targets. The sensor interface allows for a back calculation to untracked targets which is done within the radar preprocessing step. Coordinate transformation into car coordinate system is performed in this processing stage for each sensor, respectively.

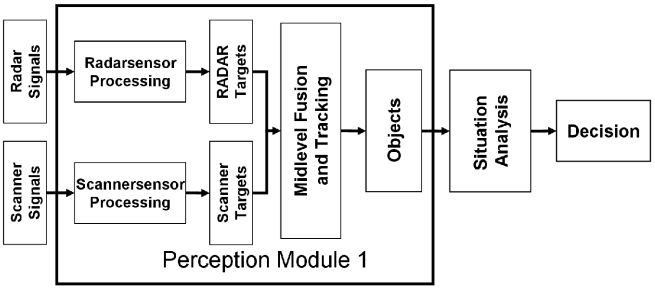

Fig. 4. System architecture. Sensor processing, fusion and tracking are realized by each module independently. The structure inside the large frame depicts the perception module 1. Situation analysis and the decision step are the same for both system approaches.

For object tracking, a standard linear Kalman filter is used [7]. The state vector of an object consists of the x- and y-position, the x- and y-component of the velocity and the orientation angle φ. Of course, the orientation angle can only be updated by laser measurements as the radar sensors deliver point targets only. Beside the estimated state, the dimension of an object and the information about which sensor has contributed measurements in the actual time cycle is stored for each object. Within the Kalman filter a linear kinematic model is used. Acceleration effects are modeled by adapting the process noise covariance. The association of measurements with tracked objects bases on a statistical distance measure. Association conflicts are resolved using the Global Nearest Neighbor (GNN) method [8] with a priority scheme based on object states. The track management distinguishes between five states of an object (in ascending order of priority): dead, initiated, tentative, missed and confirmed. There are two kinds of ambiguity that can occur when associating segments with objects: an object has more than one segment as candidate for update and a segment is a candidate for more than one object. The first ambiguity is resolved by using the GNN method. If the reference point of a segment lies within the gate of several objects, the object with higher priority gets the measurement for update. If states are equal, the dimensions of segment and objects are compared, and the segment is associated with the most similar object.

Already tracked objects, that are not confirmed in the actual time cycle are kept and will only be deleted if no corresponding object can be assigned during some cycles in succession. If on the other hand an object can not be associated with any existing track, a new one is created.

The combination of radar and laser measurements is done by a measurement vector fusion. Each component c of the combined measurement vector $\mathbf{z} = (x_z, y_z, \varphi_z)^T$ is calculated with involvement of the respective variance σ according to (1), where s is the sensor index and S the maximum number of

sensors. The fused vector serves as input to the tracking filter.

$$\mathbf{z}_c = \frac{\sum_{s=0}^{S} \frac{z_{c,s}}{\sigma_{c,s}}}{\sum_{s=0}^{S} \frac{1}{\sigma_{c,s}}} \tag{1}$$

The variance of the combined measurements results in

$$\frac{1}{\sigma_c} = \sum_{s=0}^{S} \frac{1}{\sigma_{c,s}} \tag{2}$$

Attention has to be paid when combining measurements of different sensors, as reflections can originate from different parts of an object. For the radar sensors it is unknown, where the exact reflection center is located on the object. Building an exact model of the reflectivity is difficult due to immense variations in object classes and their possible behavior. Similar to [4], we assume the reflection center to be the object's nearest point to the sensor. Before performing the fusion, the position delivered by radar(s) is corrected with the distance between the center of gravity (i.e. the reference point) and the nearest point to scanner of the corresponding segment.

Another aspect when fusing data from different sensors is the synchronization between them. In our system both the laser scanner and the radar sensors work with a frequency of 25 Hz, thus, deliver data every 40ms. Nevertheless, the exact measuring time cannot be determined. The resulting synchronization error has influence on the update step within the Kalman filter, on the one hand, but affects the association step, on the other hand. Therefore, it must be taken into account when calculating whether a measurement lies within the (statistical) gate D of a predicted object.

$$D^2 = \frac{(x_{pred} - x_{meas})^2}{\sigma_x^2} + \frac{(y_{pred} - y_{meas})^2}{\sigma_y^2} \tag{3}$$

In (3), x_{pred} and y_{pred} denote the predicted object position and x_{meas}, y_{meas} denote the position of the measurement, respectively. The total variance does not only include the process noise and measurement noise, but also a component representing the synchronization noise:

$$\begin{aligned} \sigma_x^2 &= \sigma_{x,pred}^2 + \sigma_{x,meas}^2 + \sigma_{x,sync}^2 \\ \sigma_y^2 &= \sigma_{y,pred}^2 + \sigma_{y,meas}^2 + \sigma_{y,sync}^2 \end{aligned} \tag{4}$$

where σ_{sync}^2 depends on the cycle time T and on object's velocities v (applying 3σ-method):

$$\begin{aligned} \sigma_{x,sync}^2 &= (1/3\ v_x \cdot T)^2 \\ \sigma_{y,sync}^2 &= (1/3\ v_y \cdot T)^2 \end{aligned} \tag{5}$$

In practice, the radar sensors sometimes deliver targets located outside the gate of an object but inside the object box. In this case, the information about the object being seen by this sensor is kept, but the measurement does not contribute to the fusion.

As with laser segments, ambiguities can occur in associating radar targets with existing objects. In this case, radar targets are preferably associated with objects that have laser segments already associated. If this method fails, the priority scheme as described for laser segments is applied.

IV. Perception Module 2: Cartesian Grid-based Mapping with Moving Object Detection and Tracking using MHT-IMM

This perception module was developed by the e-Motion research group of LIG laboratory and INRIA Rhône-Alpes. Different from the polar grid used in Module 1, we employ the Cartesian occupancy grid framework introduced by Elfes [9] to represent the map of subject vehicle environment. This is a stochastic spatial representation of the environment that maintains probabilistic estimates of the state of each cell occupied by an obstacle. The advantage of this approach is the ability to integrate several sensors in the same framework, taking the inherent uncertainty of each sensor reading into account.

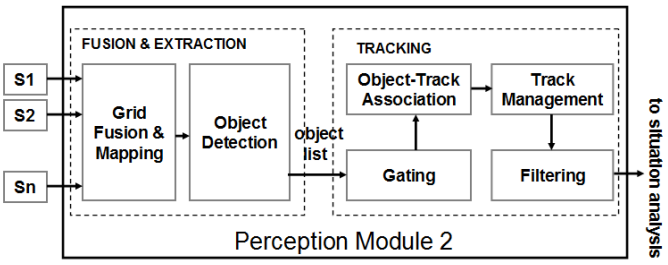

Fig. 5. The architecture of perception module 2. This replaces the large frame in Fig. 4 when running the second application variant.

Fig. 5 gives an overview of our approach which is comprised of two main parts: a) *Mapping with object detection* and b) *Object tracking*. In the first step, the occupancy grid map is constructed from sensor data sources. To correct odometry errors, we introduce a fast implementation of incremental scan matching method. After a good subject vehicle location is estimated, the grid is updated incrementally using laser measurements and moving objects are distinguished from static objects without prior knowledge of the targets. Moving objects detected by laser are then confirmed by radar measurements. Finally, we use a Multiple Hypotheses Tracker (MHT) [10] coupled with an adaptive Interacting Multiple Models (IMM) filter [11] to track detected objects and estimate their dynamic states. Final results are used as inputs for situation analysis.

In the following, we will describe in detail each step in the perception process.

A. Mapping and Object Detection

1) Mapping of the environment: In the occupancy grid framework, subject vehicle environment is divided into a two-dimensional lattice M of rectangular cells and each cell is associated with a measure taking a real value in between 0 and 1, indicating the probability that the cell is occupied by an obstacle. A high value of an occupancy grid indicates the cell is occupied and a low value means the cell is free. Assuming that occupancy states of individual grid cells are independent, the objective of a mapping algorithm is to estimate the posterior probability of occupancy $P(m|x_{1:t}, z_{1:t})$ for each cell m of grid M, given observations $z_{1:t} = \{z_1, \ldots, z_t\}$ at corresponding known poses $x_{1:t} = \{x_1, \ldots, x_t\}$.

Here we apply the Bayesian update scheme similar to that proposed in [12] which provides an elegant recursive formula to update the posterior under log-odds form:

$$\begin{aligned} log\, O(m \mid x_{1:t}, z_{1:t}) &= log\, O(m \mid x_{1:t-1}, z_{1:t-1}) + \\ &+ log\, O(m \mid z_t, x_t) - log\, O(m) \\ \text{where } O(a) &= odds(a) = P(a) \,/\, (1 - P(a)) \end{aligned} \tag{6}$$

In (6), $P(m)$ is the prior occupancy probability of the map which is initially set to 0.5 representing an unknown state, this makes this component disappeared. The remaining probability $P(m|x_t, z_t)$ is called the *inverse sensor model*. It specifies the probability that a grid cell m is occupied based on a single sensor measurement z_t at location x_t. In our implementation, it is decided by the measurement of the nearest beam to the center mass of the cell. Note that the desired probability of occupancy $P(m|x_{1:t}, z_{1:t})$ can be easily recovered from the *log odds* representation. Moreover, since the updating algorithm is recursive, it allows for incremental map updating when new sensor data arrives. Fig. 6 shows examples of an occupancy grid map where the gray color level of grid cells indicates the probability of the corresponding space being occupied: gray=*unknown*, white=*free*, black=*occupied*.

2) Vehicle Localization: In order to build a consistent map of the environment, a good subject vehicle localization is required. Because of the inherent error, using only odometry often results in an unsatisfying map. When features can not be defined and extracted, direct scan matching techniques like ICP and its variants [13] are popular ways to correct vehicle location. The most evident flaw of these ICP-style scan matching methods is that the measurement uncertainty is not taken into account. Especially, sparse data and dynamic entities in outdoor environment cause problems of correspondence finding in ICP-style methods which affect the accuracy of matching results.

An alternative approach that can overcome these limitations consists of setting up the matching problem as a maximum likelihood problem. In this approach, given an underlying vehicle dynamics constraint, the current scan's position is corrected by comparing with the local grid map constructed from all observations in the past instead of only with one previous scan. In this way we can reduce the ambiguity and weak constraint especially in outdoor environment and when the subject vehicle moves at high speeds.

Mathematically, we calculate a sequence of poses $\hat{x}_1, \hat{x}_2, \ldots$ and sequentially updated maps $M_1, M_2, \ldots$ by maximizing the marginal likelihood of the t-th pose and map relative to the $(t-1)$-th pose and map:

$$\hat{x}_t = \text{argmax}_{x_t}\{P(z_t|x_t, M_{t-1}).P(x_t|\hat{x}_{t-1}, u_t)\} \tag{7}$$

In (7), the term $P(z_t|x_t, M_{t-1})$ is the measurement model which is the probability of the most recent measurement z_t given the pose x_t and the map M_{t-1} constructed so far from observations $z_{1:t-1}$ at corresponding poses $\hat{x}_{1:t-1}$ that were already estimated in the past.

The term $P(x_t|\hat{x}_{t-1}, u_t)$ represents the motion model which is the probability that the subject vehicle is at location x_t given that the subject vehicle was previously at position $\hat{x}_{t-1}$ and executed an action u_t. The resulting pose $\hat{x}_t$ is then used to generate a new map M_t according to (8):

$$M_t = M_{t-1} \cup \{\hat{x}_t, z_t\} \tag{8}$$

For the motion model, we adopt the probabilistic velocity motion model similar to that of [12]. The vehicle motion u_t is comprised of two components, the translational velocity v_t and the yaw rate ω_t. The distribution is obtained from the kinematic equations and modeling noise of rotational and translational components. For the measurement model $P(z_t|x_t, M_{t-1})$, to avoid ray casting, we propose a method that only considers end-points of the beams. Because it is likely that a beam hits an obstacle at its end-point, we only focus on occupied cells in the grid map. For those cells, a sum proportional to the occupancy value will be voted. The final voted score represents the probability of a scan measurement z_t given the vehicle pose x_t and the map M_{t-1} constructed so far (Fig. 6). Readers could refer to [14] for more details.

Fig. 6. The subject vehicle location is obtained by trading off the consistency of laser measurement with the grid map and the vehicle ego motion.

3) Local Mapping: Because we do not need to build a global map nor deal with loop closing problem, only one online map is maintained at each point in time representing the local environment surrounding the subject vehicle. The size of the local map is chosen so that it should not contain loops and the resolution is maintained at a reasonable level. Every time the subject vehicle arrives near the map boundary, a new grid map is initialized. The pose of the new map is computed according to the subject vehicle's global pose and cells inside the intersection area are copied from the old map.

4) Moving Object Detection: After obtaining a good localization of the subject vehicle, a consistent local map is constructed. From the constructed grid, moving objects can be detected when new measurements arrive. The principal idea is based on the inconsistencies between observed free space and occupied space in the local grid map. If an object is detected in a location previously seen as free space, then it is a moving object. If an object is observed on a location previously occupied then it probably is static.

Another important clue which can help to decide whether an object is dynamic or not is the evidence about moving objects detected in the past. For example, if there are many moving objects passing through an area then any object that appears in that area should be recognized as a potential moving object. For this reason, apart from the local static map M as constructed in the previous section, a local dynamic grid map D is created to store information about previously detected

moving objects. The size and resolution of the dynamic map are the same as those of the static map. Each dynamic grid cell stores a value indicating the number of observations that a moving object has been observed at that cell.

From these remarks, our moving object detection process is carried out in two steps as follows. The first step is to detect measurements that might belong to dynamic objects. Here for simplicity, we will temporarily omit the time index. Given a new laser scan z, the corrected subject vehicle location and the local static map M and the dynamic map D containing information about previously detected moving objects, state of a single measurement z_k is classified into one of three types following: *static* if M_{hit} is occupied, *dynamic* if M_{hit} is free or $D_{hit} > \alpha$, *undecided* otherwise; where M_{hit} and D_{hit} are the corresponding cells of the static and dynamic map respectively at the end-point of the beam z_k, α is a pre-defined threshold.

The second step is performed after measurements belonging to dynamic objects are determined. Moving objects are identified by clustering end-points of these beams into separate groups, each group represents a single object. Two points are considered as belonging to the same object if the distance between them is less than 0.2 m.

Fig. 7 illustrates the moving object detection process. The leftmost image depicts the situation where the subject vehicle is moving along a street seeing a car moving ahead and a motorbike moving in the opposite direction. The middle image shows the local static map and the subject vehicle location and the current laser scan is displayed in black (resp. red) color. Measurements which fall into free region in the static map are detected as dynamic and are displayed in the rightmost image. After the clustering step, two moving objects (in boxes) are identified and correctly correspond to the car and the motorbike.

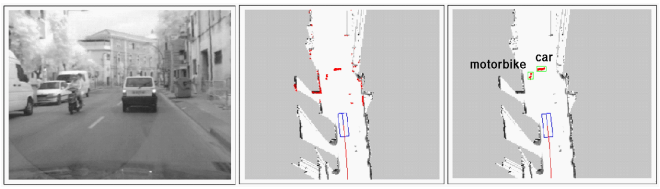

Fig. 7. Example for moving object detection. The big rectangle represents the subject vehicle.

5) Fusion with radar: After moving objects are identified from laser data, we confirm the detection results by fusing with radar data. Since data returned from radar sensors are pre-filtered as lists of potential targets, each target in the lists is provided with information about the location and the estimated Doppler velocity, the data fusion is performed at object-level.

For each object detected by laser as described in the previous section, a rectangular bounding box is calculated and the radar measurements which lie within the box region are then assigned to the corresponding object. The velocity of the detected moving object is estimated as the average of these corresponding radar measurements.

Fig. 8 shows an example of how the fusion process takes place. Moving objects detected by laser data are displayed as dots within bounding boxes. The targets detected by two radar sensors are represented as circles along with corresponding velocities. We can see in the radar field of view, two objects detected by laser data are also seen by two radars so that they are confirmed. Radar measurements that do not correspond to any dynamic object or fall into other region of the grid are not considered.

Fig. 8. Moving objects detected from laser data are confirmed by radar data.

B. Object Tracking

In the second level, moving objects detected in the vehicle environment are tracked. Since some objects may be occluded or some are false alarms or not detected, object tracking helps to identify occluded objects, recognize false alarms and reduce misdetections.

In general, the multiple object tracking problem is complex: it includes the definition of filtering methods, association methods and maintenance of the list of objects currently present in the environment. Regarding filtering techniques, Kalman filters [7] or particle filters [15] are generally used. These filters require the definition of a specific dynamic model of tracked objects. However, defining a suitable motion model is a real difficulty. To deal with this problem, Interacting Multiple Models [16] have been successfully applied in several applications. The IMM approach overcomes the difficulty due to motion uncertainty by using more than one motion model. The principle is to assume a set of models as possible candidates for the true displacement model of the object at one time. To do so, a bank of elemental filters is run at each time, each corresponding to a specific motion model, and the final state estimation is obtained by merging the results of all elemental filters according to the distribution probability over the set of motion models.

In the previous work [11], we have developed a fast method to adapt on-line IMM according to trajectories of detected objects and so we obtain a suitable and robust tracker. To deal with the data association and track maintenance problem, we extend our approach to multiple object tracking using Multiple Hypotheses Tracker [10]. The basic principle of MHT is to generate and update a set of association hypotheses during processing. A hypothesis corresponds to a specific probable assignment of observations with tracks. By maintaining and updating several hypotheses, association decisions are made and ambiguous cases are solved in further steps.

As shown in Fig. 5, our multiple object tracking method is composed of four different steps. In the first step (gating), based on predictions from previous computed tracks, we compute the set of new detected objects which can be

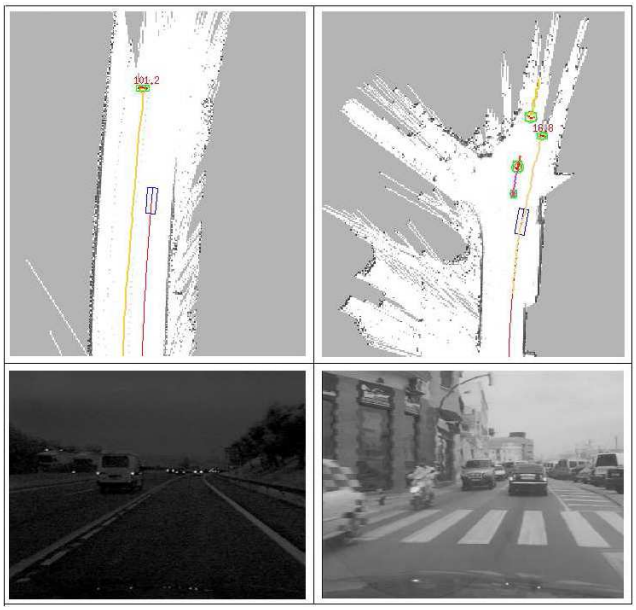

Fig. 9. Results obtained using the perception module 2 in real-life traffic with two different scenarios: on highway (at night) and on urban street.

associated with each track. In the second step, using the result of the gating, we perform object to track association and generate association hypotheses, each track corresponding to a previously known moving object. The output is composed of the computed set of association hypotheses. In the third step (track management) tracks are confirmed, deleted or created according to the association results which yield final track trees as output. With filtering in the last step, estimates are computed for "surviving" tracks and predictions are performed to be used for further process.

C. Results from perception module 2 on real-life traffic data

Fig. 9 illustrates results of the perception module 2 in two different scenarios. The upper images represent online maps and tracked moving objects in the vicinity of the subject vehicle. The current subject vehicle location is represented by a large box along with its estimated trajectories. Dots within the boxes are current laser measurements that are identified as belonging to dynamic objects. The boxes indicate detected and tracked moving objects with corresponding tracks displayed in different colors. Information on velocities is displayed next to detected objects if available. The lower images are for visual reference to corresponding situations.

On the left is a scenario where the subject vehicle is moving at a very high speed of about 100 km/h on a highway while a car moving in the same direction in front of it is detected and tracked. On the right, the subject vehicle is moving quite slowly at about 20 km/h on a crowded city street. A car moving ahead, two other cars and a motorbike moving in the opposite direction are all tracked successfully. More results and videos can be found at: http://emotion.inrialpes.fr/˜tdvu/videos/.

V. Situation Analysis and Decision

Algorithms for situation analysis and decision were developed in the framework of the APALACI project with the objective of recognizing unavoidable crash situations. They are independent from the methods and algorithms used in the perception modules.

The perception modules deliver a description of the car's environment by means of a list of objects with information about their position, movement and from which sensor(s) they originated. Subsequent steps calculate for all objects in the environment in front of the subject vehicle, whether they would potentially hit the subject vehicle according to the prediction of their movement, and the TTC, if applicable. The decision for or against an imminent collision is supported by considering statistical data about the object.

Beside the prediction of the object's velocity, the situation analysis stage is based on a data history collected for each object during its life time. In this step, a preselection is made between objects, that will potentially hit the subject vehicle and those that are most likely not hazardous or exceedingly unconfident. Only potentially dangerous objects are considered in the decision step. The most important criterion is the TTC. Objects that reach the decision step have a calculated TTC within the time frame of 200 ms which is relevant for the application. For a robust system behavior, further attributes of an object are inspected to ensure their reliability. Objects with following attributes are rejected:

- calculated point of impact is located outside the front end of the subject vehicle
- object's state is not "confirmed"
- velocity (relative to subject vehicle) too small
- object is near the border of the field of view
- too high variation of velocity and/or acceleration over time

Nevertheless, uncertainties remain due to noise in measuring and preprocessing and simplifying model assumptions. Another aspect is that any kind of sensor may deliver so-called ghost targets that do not correspond to any real-existing object. Therefore, in the decision step we have to deal with two questions:

- Will we really collide with the object?
- Does the object really exist?

For answering the first question, a Bayesian classifier is applied. Let K be the event "object collides" with the probabilities $P(K) + P(\neg K) = 1$. Then, the probability of a collision given a certain measurement z is

$$P(K|z) = \frac{P(K,z)}{P(z)} \tag{9}$$

Applying Bayes rule, this is the same as

$$\begin{aligned} P(K|z) &= \frac{P(z|K)P(K)}{P(z)} \\ &= \frac{P(z|K)P(K)}{P(z|K)P(K) + P(z|\neg K)P(\neg K)} \end{aligned} \tag{10}$$

where z is composed of different attributes z_i: the variance of the x-component of the velocity, the lifetime of the object and the number of cycles the object was categorized as critical. To judge the criticality of an object, it is inspected within a

determined time period that is longer than the TTC. Assuming independent attributes z_i and, furthermore, K and $\neg K$ equiprobable, the probability of a collision can be calculated using (11).

$$P(K|z) = \frac{\prod P(z_j|K)}{\prod P(z_j|K) + \prod P(z_j|\neg K)} \tag{11}$$

The conditional probabilities $P(z_j|K)$ and $P(z_j|\neg K)$ are determined beforehand in an offline procedure by inspecting numerous examples with different situations. Finally, an object is considered as crashing object if $P(K|z)$ exceeds a predefined threshold.

Beside the probability of a collision, the probability of existence has to be considered in order to prevent false alerts that may arise from ghost targets delivered by the sensors or failures in associating measurements with objects. We use a method based on evidence theory introduced by Dempster and Shafer [17] [18].

For a classification of existing and non-existing objects we define the hypothesis space as $\Theta = \{E, \neg E\}$ where E stands for "object exists" and $\neg E$ stands for "object does not exist". In evidence theory the power set $2^\Theta = \{\emptyset, E, \neg E, E \cup \neg E\}$ is considered. Sensor-specific mass functions assign probability masses to the elements in the power set. For the laser scanner, the mass functions are implemented as:

$$\begin{aligned} m_l(E \cup \neg E) &= c_l \\ m_l(E) &= \frac{\sum_{i=0}^{N} 2^{N-i} \cdot h_l[i]}{\sum_{i=0}^{N} 2^{N-i}} \cdot (1 - m_l(E \cup \neg E)) \\ m_l(\neg E) &= 1 - (m_l(E) + m_l(E \cup \neg E)) \end{aligned} \tag{12}$$

By definition, $m_l(\emptyset) = 0$. The constant term c_l denotes a mass probability for uncertainty. The mass function for the hypothesis "object exists" considers the weighted ratio of the number of detections to the lifetime of an object within a given time frame N. In this connection, $h_l[i]$ contains the information about the object being detected by the laser scanner at time i. Younger data is exponential higher weighted than older data. The remaining mass for the hypothesis "object does not exist" is derived from the condition

$$\sum\nolimits_{X \subseteq \Theta} m(X) = 1 \tag{13}$$

Mass functions for radar sensors are implemented in an analogous way. The fusion of masses from the different sensors is performed in two steps. First, the masses from the two radar sensors are combined. Second, the resulting radar masses are combined with the masses calculated for the laser scanner. For fusion, Dempster's combination rule is used [18].

The final step of the decision module combines the probability of collision that is provided by the Bayes classifier with the probability of existence. For the Bayes classifier we define the hypothesis space $\Theta = \{C, \neg C\}$ with the hypothesis C for a colliding object and $\neg C$ for a non-colliding object. The probability masses $m_b(C)$ and $m_b(\neg C)$ are directly taken from the conditional probabilities for K (see (11)).

$$\begin{aligned} m_b(C) &= P(K|z) \\ m_b(\neg C) &= P(\neg K|z) = 1 - m_b(C) \\ m_b(C \cup \neg C) &= 0 \end{aligned} \tag{14}$$

In this case, the uncertainty $C \cup \neg C$ is equal to zero, because Bayesian probabilities do not provide a measure for uncertainty. For the interesting case "object exists and collides" the combined probability mass results in

$$m_f(E \cap C) = m_b(C) \cdot (m_c(E) + m_c(E \cup \neg E)) \tag{15}$$

If m_f exceeds a predefined threshold, actuators are triggered.

In general, laser measurements are able to describe the position and shape of real existing objects very accurately. Radar sensors help to suppress ghost targets or targets based on objects that are irrelevant for precrash applications like plants or steam coming out of street drains. All in all, the presented precrash system based on a laser scanner fused with short range radars reliably detects different kinds of collisions with stationary objects in front of the car, as our evaluation in Section VI shows.

VI. Experimental Results

The application has been validated in complex crash and non-crash scenarios. To conduct the experiments, we built up a comprehensive database that consists of short sequences of measurements recorded during predefined driving maneuvers. These maneuvers comprise factual and near missed collisions with stationary objects at different velocities, in curves, with deceleration, sudden lane changes and lane changes of a leading target vehicle obstructing the sight to the obstacle. In the maneuvers, foam cubes and cylinders served as crash objects. To measure the quality, we counted the false alarms that occurred in non-crash scenarios and the missed alarms in case a collision was not detected by the application. Table II compares the results for the non-crash scenarios for the two different modules and Table III lists the results for the crash scenarios.

As a general result it can be stated that a reliable collision detection is achieved with both perception modules. Whereas Module 1 enables a lower false alarm rate, the crash detection rate of Module 2 is very high (98.1%). The three false alarms in the scenario where we pass the cylinder in a curve occurred in cases of getting extremely close to the obstacle. In contrast, no false alarms occurred at all when the subject vehicle suddenly changes the lane to avoid a collision with an obstacle standing on the road. Emergency brake maneuvers challenge the tracking system because of the divergent motion scheme. In our evaluation, only 1 out of 19 test drives resulted in a false alarm for each module.

In motion estimation, there is always a tradeoff between stabilization of the current state and the adaptation to dynamic situations. It becomes apparent when looking at the scenarios where the system fails. In case of cornering, for example, the direction of the obstacle's relative movement continuously changes. From the results in curve scenarios, it can be seen, that the two modules handle such situation in a different way. Module 2 produces more false alarms, whereas Module 1 risks more missed alarms. Looking at Table III, missed alarms provoked by Module 1 are overrepresented in high speed scenarios. An object with a high relative velocity is

TABLE II
RESULTS FOR COMPLEX NON-CRASH SCENARIOS

Scenario	Ego velocity [km/h]	Number of tests	False alarms/False alarm rate	
			Module 1	Module 2
Near-missed passing of cylinder	40, 60	9	0 / 0%	0 / 0%
Near-missed passing of cube	40, 60	6	0 / 0%	0 / 0%
Near-missed passing of cylinder after curve (45°)	40, 60	29	0 / 0%	3 / 10.3%
Emergency brake, distance to cylinder after brake not greater than 1.5 m	40, 60 (at start)	19	1 / 5.3%	1 / 5.3 %
Lane change maneuver to avoid a collision with a cube	30, 40, 50, 60, 70	22	0 / 0%	0 / 0%
Gate passing	30, 50	6	0 / 0%	0 / 0%
Gate passing after curve (45°)	30, 50	4	0 / 0%	0 / 0%
Total		**95**	**1 / 1.1%**	**4 / 4.2%**

TABLE III
RESULTS FOR COMPLEX CRASH SCENARIOS

Scenario	Ego velocity [km/h]	Number of tests	Missed alarms/Missed alarm rate	
			Module 1	Module 2
Collision with cylinder, varying points of impact	20, 40	24	0 / 0%	0 / 0%
Collision with (paper) cylinder at high speed, varying points of impact	60, 120	8	2 / 25.0%	0 / 0%
Collision with cube, point of impact has high offset	40	7	0 / 0%	1 / 14.3%
Collision with cylinder after curve (30°, 45°)	30, 40, 60	20	2 / 10.0%	0 / 0%
Collision with cylinder or cube after emergency brake	20, 40 (at crash time)	7	0 / 0%	0 / 0%
Collision with (paper) cylinder after emergency brake at high speed	60, 80 (at crash time)	9	2 / 22.2%	0 / 0%
Collision with cylinder after lane change maneuver	40, 50	23	1 / 4.3%	1 / 4.3%
Collision with cylinder after leading car lane change	40, 50	4	0 / 0%	0 / 0%
Total		**102**	**7 / 6.9%**	**2 / 1.9%**

registered infrequently during the time period available for creating a data history for this object as described in Section V. In this case, the decision is supported by less data. Depending on the influence of new measurements on the current state, the grid map approach may be advantageous over a single frame processing realized in Module 1, in this special case. In general, it should be highlighted that a lot of the test maneuvers have been performed at the vehicle dynamics limit.

In a third experiment we tested the application in normal traffic on highways, rural roads and in urban areas. To achieve representative results we performed the test drives during day time to cover different traffic situations like rush hour, traffic jam and stop-and-go. Furthermore, the test drives were partly conducted under adverse weather conditions like rain, fog, wet roads and traffic spray. All in all, we covered a distance of 1600 km, running the application in real time. This test was performed within the framework of the APALACI project using the perception module 1 only. There were no wrongly detected collisions in any of these environments.

VII. CONCLUSION AND OUTLOOK

In this paper we compared two approaches that perform the data processing and object generation fusing laser scanner and short range radar sensors. The obtained description of the vehicle's environment in terms of static and moving objects serves as a basis for safety systems that trigger restraint systems in case an unavoidable collision will take place.

Comprehensive tests show, that a good detection performance for frontal collisions is achieved with both approaches. Comparing the results of both approaches, the sums of false and missed alarms balance each other. The application was running stably in a hard real-time environment and has been extensively tested in real traffic scenarios and with artificial crash and near crash maneuvers carried out on test tracks. The function has been successfully demonstrated in a public event during the 2007 PReVENT IP Exhibition in Versailles and at the IEEE Intelligent Vehicles Symposium, 2008, in Eindhoven.

Future works will extend the perception modules in order to improve the detection of collisions with moving objects and with the major goal to shift the activation decision to a time earlier than 200ms. This includes the refinement of motion models and object models to give a more meaningful representation of detected objects with specific shapes and behavior.

REFERENCES

[1] A. Vahidi and A. Eskandarian, *Research Advances in Intelligent Collision Avoidance and Adaptive Cruise Control*, IEEE Trans. Intell. Transp. Syst., vol. 4, nr. 3, 2003, pp.143-153.

[2] J. Hillenbrand, A. M. Spieker and K. Kroschel, *A Multilevel Collision Mitigation Approach–Its Situation Assessment, Decision Making, and Performance Tradeoffs*, IEEE Trans. Intell. Transp., vol. 7, nr. 4, 2006, pp. 528-540

[3] R. Labayrade, C. Royere and D. Aubert, *A Collision Mitigation System using Laser Scanner and Stereovision Fusion and its Assessment*, Proc. IEEE Intell. Veh. Symp., 2005, pp. 441-446

[4] S. Wu, S. Decker, P. Chang, T. Camus and J. Eledath, *Collision Sensing by Stereo Vision and Radar Sensor Fusion*, Proc. IEEE Intell. Veh. Symp., 2008, pp. 404-409

[5] M. Skutek, D.T. Linzmeir, N. Appenrodt and G. Wanielik, *A Precrash System based on Sensor Data fusion of Laser Scanner and Short Range Radars*, Proc. IEEE Int. Conf. on Inform. Fusion, 2005, pp. 1287-1295.

[6] D. Streller and K. Dietmayer, *Object Tracking and Classification Using a Multiple Hypothesis Approach*, Proc. IEEE Intell. Veh. Symp., 2004, pp. 808-812
[7] R.E. Kalman, *A New Approach to Linear Filtering and Prediction Problems*, in Transactions of the ASME-Journal of Basic Engineering, 1960, vol. 82, pp. 35-45.
[8] Y. Bar-Shalom and T.E. Fortmann, *Tracking and Data Association*, Orlando, Academic Press, 1988.
[9] A. Elfes, *Occupancy grids: a probabilistic framework for robot perception and navigation*, Ph.D. dissertation, Carnegie Mellon Univ., 1989.
[10] S.S. Blackman, *Multiple hypothesis tracking for multiple target tracking*, IEEE Aerosp. Electron. Syst. Mag., 19 (1), 2004, pp. 5-18.
[11] J. Burlet, O. Aycard, A. Spalanzani and C. Laugier, *Adaptive Interactive Multiple Models applied on pedestrian tracking in car parks*, in Proc. IEEE Int. Conf. on Intelligent Robots and Systems, 2006, pp. 525-530.
[12] S. Thrun, W. Burgard, and D. Fox, *Probabilistic Robotics (Intelligent Robotics and Autonomous Agents)*, The MIT Press, September 2005.
[13] S. Rusinkiewicz and M. Levoy. *Efficient variants of the icp algorithm*, 2001.
[14] T.D. Vu, O. Aycard, and N. Appenrodt, *Online localization and mapping with moving object tracking*, in Proc. IEEE Intelligent Vehicles Symposium, Istanbul, 2007, pp. 190-195.
[15] S. Arulampalam, S. Maskell, N. Gordon, T. Clapp, *A tutorial on particle filter for online nonlinear/non-gaussian bayesian tracking*, IEEE Transactions on Signal Processing, 50 (2).
[16] E. Mazor, A. Averbuch, Y. Bar-Shalom, J. Dayan, *Interacting multiple model methods in target tracking: a survey*, IEEE Transactions on Aerospace and Electronic Systems, 34 (1), 1998, pp. 103123.
[17] G. Shafer, *A mathematical theory of evidence*, Princeton University Press, 1976.
[18] A. Dempster, *A Generalization of Bayesian Inference*, in Journal of the Royal Statistical Society, vol. 30, 1968, pp. 205-247.

Sylvia Pietzsch received her diploma in Computer Science from the Technische Universität München, Germany, in 2007. Currently, she is with the Chair for Image Understanding and Knowledge-based Systems of the Technische Universität München as a doctoral candidate. She pursues her studies at the Daimler AG, Department for Environment Perception. Her research interests include sensor data processing and fusion for driver assistance systems.

Trung Dung Vu is a PhD candidate at INRIA Rhne-Alpes Grenoble since 2006. He received his BSc from the Faculty of Technology, Vietnam National University in 2001 and his MSc from the Institute National Polytechnique de Grenoble (INPG) in 2005. His research interests include range sensor processing, computer vision and machine learning.

Julien Burlet obtained his PhD in Mathematics and Computer Science from the Institute National Polytechnique de Grenoble (INPG), France in 2007. His knowledge and interest in machine learning and autonomous systems is demonstrated by more than ten publications in this field addressing localisation, multiple object tracking and classification. In 2008, Julien Burlet joined TRW-Conekt, Solihull, UK as a research and development engineer. Since then, he pursued his research on object detection, tracking and classification with radars and cameras while focusing on Automotive and Ministry of Defence applications.

Olivier Aycard received his PhD in Computer Science from the University of Nancy in 1998. In 1999, he was visiting researcher at Nasa Ames Research Center in Moffett Field, CA. Since 2000, Olivier Aycard is an Associate Professor at University of Grenoble. His researches focus on Bayesian techniques for perception with an emphasis on multi-objects tracking using multi-sensor approaches. He has more than 40 publications in this field. He was also involved in several national and european projects in collaboration with european car manufacturers (Daimler, VW, Volvo, Peugeot). In addition, he is in charge of lectures in Artificial Intelligence and Autonomous Robotics at University of Grenoble.

Thomas Hackbarth was born on August 28, 1958 in Stade, Germany. He received the Diploma and PhD degrees in electrical engineering from the Technical University of Braunschweig, Germany in 1986 and 1991, respectively. In 1991, he joined the Research and Technology department of the Daimler AG in Ulm, Germany. After several years of semiconductor technology research, he changed his field of activity to the development of active and passive safety systems.

Nils Appenrodt received the Diploma degree (Dipl.-Ing.) in electrical engineering from the Universität Duisburg, Germany, in 1996. He was research assistant in the field of imaging radar systems at the Universität Duisburg working in close cooperation with DaimlerChrysler research institute, Ulm. Since 2000 he has been with Daimler AG, Group Research, Ulm, mainly working on environment perception systems. His research interests include radar and laser sensor processing, sensor data fusion and safety systems.

Jürgen Dickmann is Manager Near Range Sensing at DAIMLER Research and Pre-Development. He is responsible for the development of sensors and algorithms for environmental perception in driver assistance- and safety systems. After studying electrical engineering at University of Duisburg, he started as Project Manager for high frequency devices and integrated circuits at AEG-Telefunken. In 1991 he made his PhD at RWTH Aachen as external candidate. Between 2005 and 2007 he was in charge of teams developing sensor technologies, sensor fusion- and situation analysis concepts. Since 1999 he and his team develop solutions with a focus on Pre-Crash/Pre-Safe functions at DAIMLER.

Bernd Radig received a degree in Physics from the University of Bonn in 1973 and a doctoral degree as well as a habilitation degree in Informatics from the University of Hamburg in 1978 and 1982, respectively. Until 1986 he was an Associate Professor at the Department of Computer Science at the University of Hamburg, leading the Research Group Cognitive Systems. Since 1986 he is a full professor at the Department of Computer Science of the Technische Universiät München. His research interests include Artificial Intelligence, Computer Vision, and Image Understanding, and Pattern Recognition.